Dalton Transactions

Accepted Manuscript

ROYAL SOCIETY OF CHEMISTRY

www.rsc.org/dalton

Journal Name

RSCPublishing

ARTICLE

Molecular excitons in a copper azadipyrrin complex

Cite this: DOI: 10.1039/xoxxoooooox

T. M. McLean,[a] S. G. Telfer,[a] A. B. S Elliott,[b] K. C. Gordon,[b] M. Lein[c] and M. R. Waterland*[a]

Received ooth January 2012,
Accepted ooth January 2012

DOI: 10.1039/xoxxoooooox

www.rsc.org/

Exciton coupling is investigated in a copper azadipyrrin complex, **Cu(L-aza)$_2$**. Exciton coupling in **Cu(L-aza)$_2$** assuming a single π-π* state on the **L-aza** ligand fails to account for the electronic structure of **Cu(L-aza)$_2$**, which displays two almost equal intensity transitions at 15 600 cm^{-1} and 17 690 cm^{-1}. TD-UB3LYP/6-31G(d) calculations suggest multiple π-π* transitions for the **L-aza** ligands and simple vector addition of the transition dipoles predicts two nearly orthogonal co-planar excitonic transitions that correctly reproduce the absorption band profile. Empirical modelling of absolute resonance Raman intensities using wavepacket dynamics confirms **Cu(L-aza)$_2$** has two equal intensity orthogonal exciton transitions. The phenyl substituents at the α- and γ-positions of the pyrrole rings play a central role in determining the orientation of the transition dipoles. Consequently the π-π* transitions for the **L-aza** ligands are oriented towards the substituent groups and are not in the plane of the pyrrole rings. Mode displacements in the Franck-Condon (FC) region obtained from the wavepacket model suggest that pyrrole ring and phenyl modes control the exciton FC dynamics. Our results suggest that **Cu(L-aza)$_2$** is an ideal model for theoretical, computational and experimental investigations of molecular excitons in molecular systems.

Introduction

The combination of desirable spectroscopic properties and versatile synthetic chemistry has generated considerable interest in dipyrrins and their aza- analogues in recent years.[1, 2] The core dipyrromethene structure provides π-π* transitions with very large molar absorption cross-section in the visible wavelength range which leads to excellent scattering cross-sections; derivatives with coordinated pyrrole rings, such as BODIPY™ have excellent emission quantum yields,[3, 4] whilst the neutral uncoordinated dipyrrin has very strongly enhanced resonance Raman cross-sections.[5] Azadipyrromethene complexes have attracted interest due to low energy transitions generating strong absorption and emission in the near infrared,[6-10] and as potential n-type charge-carrier materials.[7, 11]

(Aza)dipyrrins exhibit rich coordination chemistry with a wide variety of transition metal species.[7, 12-19] In transition metal species with multiple (aza)dipyrrin ligands, the large transition dipole moment of the π-π* generates coupling between the π-π* states which leads to the formation of excitonic states in metallodipyrrin species.[20-22]

Exciton coupling theory assumes dipole-dipole coupling between the π-π* states of the chromophores.[23] The relative orientation (Figure 1) of the chromophores determines the energies and oscillator strengths of the excitonic states. However, if the coupling strongly perturbs the electronic structure of the chromophores then the electronic structure is more generally described as a manifold of delocalized π-π* states. These delocalized states will resemble exciton states but the simple dependence of the energies and oscillator strengths on the geometrical parameters is lost.

In this work we consider the electronic structure of a copper tetraphenylazadipyrrin compound (**Cu(L-aza)$_2$**, Figure 1). The electronic absorption spectrum of **Cu(L-aza)$_2$** has been reported previously,[12, 17, 24] and appears anomalous compared to other **M(L-aza)$_2$** species, with two intense bands with nearly identical oscillator strength. Furthermore, applying exciton coupling theory using structural parameters (such as dihedral angle) to calculate energy splittings and intensities fails to account for the equal intensities observed in the **Cu(L-aza)$_2$** spectrum. To the best of our knowledge, a satisfactory explanation of the electronic structure of **Cu(L-aza)$_2$** has not appeared and in general the nature of excitonic interactions in azadipyrromethene compounds has not been examined. The aim of this work is to determine if the electronic states of **Cu(L-aza)$_2$** are properly described as excitonic or as delocalized π-π* states.

We use electronic structure calculations and resonance Raman spectroscopy to characterize the exciton states in **Cu(L-aza)$_2$**, and examine the cause of the apparent failure of the exciton theory for the copper azadipyrrin system. There are two simple possibilities; the wrong parameters are being used within the exciton coupling model and/or strong coupling may be present, in which case the electronic structure is more correctly described as a manifold of π-π*

excited states, rather than excitonic states. To proceed we employ electronic structure calculations to identify the components of the transition dipole moment vectors and apply exciton coupling theory using these components.

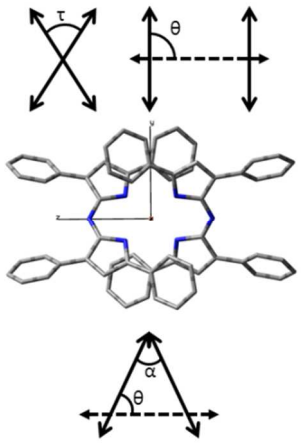

Figure 1. **Top**. Definition of θ and τ for non-planar dipoles, following ref. 7. The "line of ligand centres" (dashed arrow) and the dipole vector define the dihedral planes and τ is the dihedral angle between these planes. **Middle.** The calculated structure of **Cu(L-aza)$_2$** (with hydrogen atoms omitted for clarity). The z-axis is the line of ligand centres. **Bottom.** θ and α for co-planar dipoles. The line of ligand centres (shifted for clarity) still defines θ and α is the angle between the dipoles.

We use resonance Raman spectroscopy as a detailed probe of the nature of the excitonic states. The resonant enhancement of the Raman mode intensities depends strongly on the nature of electronic states. Interference between Raman scattering from multiple excitonic states allows the orientation of the exciton transition dipoles to be determined by fitting an empirical model of wavepacket dynamics to experimental absolute resonance Raman cross-sections.

The wavepacket model also provides a description of the nuclear dynamics in the Franck-Condon state.[25] Previous resonance Raman studies of metallodipyrrin compounds have shown that Franck-Condon dynamics directly influence excited-state lifetime and emission properties and the substituent at the meso- position plays a critical role in determining Franck-Condon dynamics in dipyrrin compounds.[26] In this work we identify the key structural features that control Franck-Condon dynamics in **Cu(L-aza)$_2$**. The quantitative resonance Raman cross-sections presented here will also provide valuable experimental data for validating recently introduced ab initio and DFT methods for the calculation of resonance Raman intensities in complex molecules.

Experimental, Computational and Theoretical Details

Cu(L-aza)$_2$, was synthesized according to literature methods[17] and spectroscopic data matched those previously reported. Solvents were spectroscopic grade (Sigma-Aldrich) and were used as received. Absorption spectra were recorded on a Shimadzu U-3101 spectrometer. Raman spectra were collected in dichloromethane solution at various concentrations ranging from 0.5 mM to 5 mM (depending on excitation wavelength). Raman instrumentation, parameters, data collection, and data analysis have been described in detail elsewhere.[5, 25, 26] Computational chemistry was performed using the Gaussian09 suite,[27] using an unrestricted B3LYP/6-31G(d) model and a C-PCM solvent model to obtain optimized geometry and frequencies, and the corresponding TD-UB3LYP method was used to determine transition dipoles and excited state energies.

Absolute Raman cross-sections and absorption cross-sections were modeled using empirical wavepacket methods and the details of this model have been published previously.[28, 29] For the **Cu(L-aza)$_2$** system, two electronic states were included in the model and the angle between transition dipoles was included as a parameter. Vibrational modes were assumed to be separable and Duchshinsky rotation effects were not included. The solvent was modeled using Mukamel's Brownian Oscillator model.[30]

Results and discussion

Exciton Splitting Energy

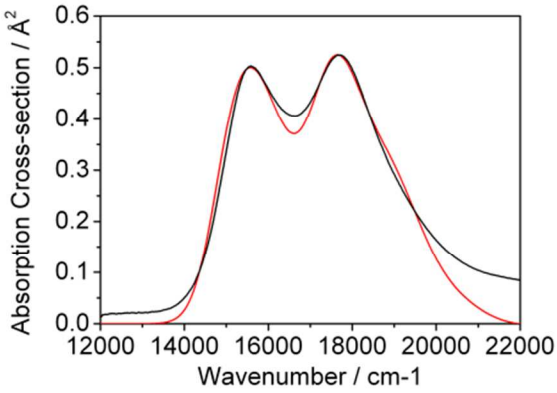

Figure 2. Experimental absorption spectrum (black trace) for **Cu(L-aza)$_2$** in CH_2Cl_2. The red trace shows the absorption spectrum simulated using wavepacket dynamics.

The absorption spectrum is shown in Figure 2 (using an energy scale) and in Figure 3 (using a wavelength scale). The exciton splitting energy is 2140 cm^{-1} for **Cu(L-aza)$_2$**. If we assume the transition dipole lies within the plane of the dipyrromethene core then the two-fold ligand symmetry requires $\theta = 90^o$. We calculate the exciton splitting energy using

$$\Delta E = \frac{2|M|^2}{r^3}(cos\,\tau - 3cos^2\theta).$$

For $\tau \neq 0$ the dipoles are non-planar, and the exciton splitting energy is determined by the dihedral angle, τ. We compare the

previously reported zinc complex of L-aza,[31] for which $\tau = 63.5^o$, with **Cu(L-aza)$_2$**. The dihedral angle of **Cu(L-aza)$_2$** is 48°;[17] this difference in dihedral angle increases the exciton splitting energy in **Cu(L-aza)$_2$** by a factor of 1.58 (assuming the transition dipole moment, M, and distance between chromophores, r, are approximately equal for the copper and zinc complexes). The zinc complex shows a strong peak at 16 900 cm^{-1} and a weak shoulder at 15625 cm^{-1}, giving a splitting of 1290 cm^{-1}. The ratio of observed splitting energies, 2140 cm^{-1}/1290 cm^{-1} = 1.65, is not dissimilar from that predicted using the geometrical dihedral angle. Although this analysis approximately accounts for the energy splitting (for the wrong reasons) it fails entirely to predict the intensities of the bands for **Cu(L-aza)$_2$**, as the oscillator strength can only be carried by one of the exciton transitions for non-planar transition dipoles.[23]

Table 1. Experimental and calculated transition energies, oscillator strengths (***f***) and transition dipole moment coordinates (***x, y, z***).

Experimental		Calculated				
ν / cm^{-1}	***f***	**ν** / cm^{-1}	***f***	***x***	***y***	***z***
15 600	0.143	16 690	0.10	0.0	0.0	1.4
17 690	0.204	17 180	0.32	2.5	0.0	0.0
		18 020	0.49	0.0	−3.0	0.0
		18 520	0.10	0.0	0.0	1.4
		18 550	0.64	0.0	+3.4	0.0

TD-DFT Results and Exciton Transition Intensities

For non-planar dipoles ($\theta = 90^o$, $\tau \neq 0$), the exciton coupling theory predicts only one of the exciton transitions is allowed.[22, 23] The copper complex shows two exciton bands with equal intensity and it is the origin of these intensities that must be established. Implicit in the exciton model is the excited state manifold of each chromophore (or each ligand for **Cu(L-aza)$_2$**) is dominated by a single excited state. For the azadipyrrins, our computational results suggest a more complicated picture. Calculated excited-state energies, transition dipole coordinates and oscillator strengths are presented in Table 1, and shown in Figure 3. Structural parameters, and calculated frequencies (supplementary information) show good agreement with experimental data. Due to the D_2 symmetry of **Cu(L-aza)$_2$** , π-π* transitions for the individual ligands cannot be identified. There are five states with sufficient oscillator strength to exhibit dipole-dipole coupling. The transition dipoles for these states are oriented along the C_2 symmetry axes (which coincide with the Cartesian axes), shown in Figure 4. There are two transition dipoles oriented along the $C_2(z)$ and $C_2(y)$ axes, and one dipole along the $C_2(x)$ axis with sufficient magnitude for dipole-dipole coupling. The $C_2(y)$ dipoles have a larger magnitude ($f \approx 0.5$) than the $C_2(z)$ dipoles ($f \approx 0.1$) and the $C_2(x)$ dipole has an intermediate magnitude ($f \approx 0.3$). Note the $C_2(z)$ dipoles have the same magnitude and direction.

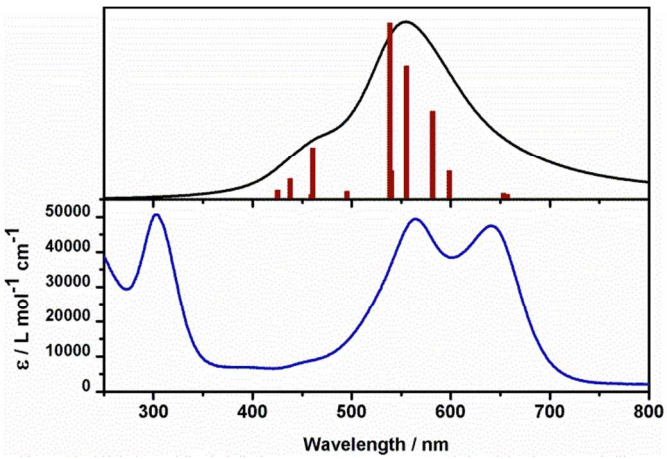

Figure 3. Top, transition energies and oscillator strengths from TD-UB3LYP/6-31G(d) calculation. **Bottom**, experimental absorption spectrum.

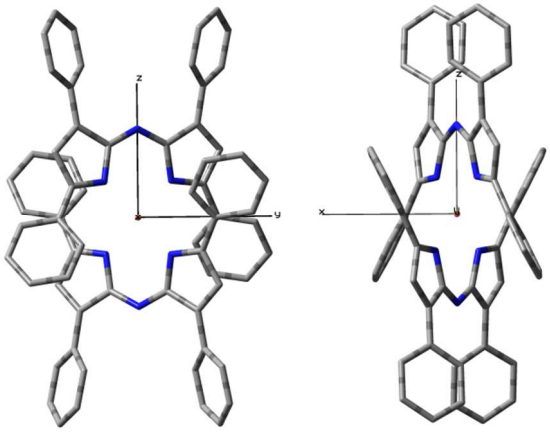

Figure 4. Calculated structures for **Cu(L-aza)$_2$**. Hydrogen atoms have been omitted for clarity. Views are shown looking down the *x* (left) and y (right) axes. The calculated dihedral angle, τ, is 56°.

We now demonstrate that vector addition of the transition dipoles shown in Table 1 creates two resultant dipoles that are co-planar but not parallel. In this case the relevant expressions for the exciton splitting energy and transition dipole magnitude are

$$\Delta E = \frac{2|\boldsymbol{M}|^2}{r^3}(\cos\alpha + 3\cos^2\theta)$$

$$\boldsymbol{M}' = \sqrt{2}\boldsymbol{M}\cos\theta$$

$$\boldsymbol{M}'' = \sqrt{2}\boldsymbol{M}\sin\theta$$

For simplicity, the addition of the $C_2(y)$ and $C_2(z)$ dipoles is described first. θ is defined using the "line that joins the ligand centres". Considering only the *y*- and *z*- components this line is the *z*-axis. Vector addition using the values in Table 1 gives two *co-planar* resultant dipoles in the *yz*-plane with $\theta \approx 67.5^o$ and $\alpha \approx 45^o$. Extending this analysis to include the $C_2(x)$ dipole, note that the

line of ligand centres† must lie in the *xz*-plane, and also in the plane of the final resultant dipoles. The plane containing the final exciton dipoles makes an angle of approx. 60.7^o with the *yz*-plane, and we find $\theta \approx 48^o$ and $\alpha \approx 86^o$for the final exciton dipoles. The calculated dipole magnitudes are approximately equal and our analysis shows there are two exciton transitions with approximately equal intensity ($\boldsymbol{M''/M'} = 1.1$). We conclude from this analysis that exciton coupling theory does hold for the **Cu(L-aza)$_2$** system, but the transition dipoles are not simply related to structural elements. In **Cu(L-aza)$_2$** , dipole-dipole coupling generates co-planar dipoles in an orientation that distributes intensity almost equally to both exciton states. The plane of the exciton transition dipoles no longer coincides with the plane of the pyrrole rings. Considering the analysis of the exciton splitting energies above, it is merely good fortune that the parameters obtained from the structural data provide an exciton splitting energy in good agreement with the experimental data. The TD-DFT calculations provide the relative orientation (and magnitude) of the transitions dipoles, which allows $\boldsymbol{M''/M'}$ to be determined, but not the separation, r, between the dipoles. The exciton energy splitting cannot therefore be determined from the TD-DFT output alone.

Although **Cu(L-aza)$_2$** appears somewhat anomalous compared to other homoleptic L-aza complexes,[13, 16, 17, 31] there are examples of excitonically coupled dipyrrin chromophores that exhibit a clearly defined doublet in their electronic absorption spectra.[32-34] Broring *et al* have synthesized covalently coupled BODIPY dimers with absorption spectra that resemble the **Cu(L-aza)$_2$** spectrum and the dipyrrin chromophores are also co-planar in these systems. The co-planar orientation of the dipyrrin transition dipoles leads to a similar intensity distribution as the co-planar exciton dipoles for **Cu(L-aza)$_2$**.

The calculated excited state transitions are described by multiple configurations which complicates the interpretation, but a qualitative description of the transitions can be obtained from the Kohn-Sham (KS) orbitals (supporting information); the *z*-polarised transitions originate on orbitals localized on the γ-phenyl substituents and terminate on orbitals including the pyrrole ring atoms and bridging nitrogen atoms; the *x*-polarised transition originates on orbitals involving pyrrole atoms and terminates on the orbitals of the phenyl groups at the α-positions; the *y*-polarised transitions also originate on orbitals localized on the γ-phenyl substituents and terminate on orbitals including the pyrrole ring atoms and bridging nitrogen atoms. It is clear that the phenyl substituents strongly influence the electronic transitions in **Cu(L-aza)$_2$**. In **Cu(L-aza)$_2$**, at least, the exciton transition dipoles, whose coordinates are shown in Figure 5, are oriented toward the phenyl rings and away from the plane of the pyrrole rings.

B3LYP is known to have difficulties predicting spectroscopic properties of systems with extended π-systems and charge-transfer transitions.[35-37] The TD-B3LYP transitions calculated for **Cu(L-aza)$_2$** are the result of the short-range correlation effects included in the B3LYP model. It is therefore not surprising that the TD-B3LYP method does not completely account for the observed excitonic interactions.[38, 39] By taking the TD-B3LYP transition dipoles and

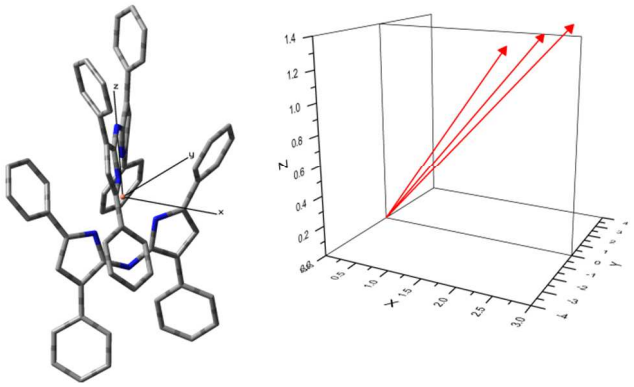

Figure 5. Orientation of the resultant exciton dipoles relative to molecular structure. The line of ligand centres lies in the *xz*-plane at $y = 0$, and makes an angle of 60.7^o with the *yz*-plane.

semi-quantitatively accounting for long-range dipole-dipole coupling *ex post facto* we obtain excellent agreement with the experimental data. We believe the excitonic states in **Cu(L-aza)$_2$** provide an ideal proving ground for more sophisticated ab initio treatments of azadipyrrin excited states[40-42] that were beyond the scope of the current work.

The alternative explanation, *i.e.* strong coupling or delocalization across the azadipyrrin ligands, would be mediated by orbital overlap. There is minimal amplitude on the copper atom in the frontier orbitals in **Cu(L-aza)$_2$** which suggests that delocalisation is not responsible for the electronic structure in **Cu(L-aza)$_2$**. π-π interactions between the phenyl substituents may also mediate coupling between the ligands. Using a recent study of the magnitude of π-π interactions in benzene dimers[43] we estimate the interaction energy between the phenyl substituents of **Cu(L-aza)$_2$** to be < 400 cm^{-1}, well below the experimentally observed splitting energy. It is likely that π-π interactions are present but do not dominate the coupling between the ligands in **Cu(L-aza)$_2$.**

Resonance Raman spectra and wavepacket modelling

The resonance Raman spectra of **Cu(L-aza)$_2$** are shown in Figure 6. Variations in band intensities are observed as excitation is moved across the exciton states. These variations are shown more clearly in the Raman excitation profiles (data points) in Figure 7.

Wavepacket dynamics were used to simulate the resonance Raman intensities and absorption spectrum.[44] The excited-state structure was modelled with two excited states, X_1 and X_2; the parameters for each state included excited-state energy, E_{00}, transition dipole length, μ, and relative orientation of the transition dipoles, α (as defined in Figure 1), along with parameters to describe the solvent interaction.[30] These empirical parameters are varied to obtain resonance excitation profiles and an absorption spectrum that best fit the experimental data. The best fit absorption spectrum is shown in Figure 2. Figure 7 shows simulated Raman excitation profiles and the absolute differential Raman cross-sections used to fit the excitation profiles. Selected optimized parameters are shown in Table 2 and Table 3. The Raman profiles were simulated for a range of α values. For resonant Raman scattering from two states,

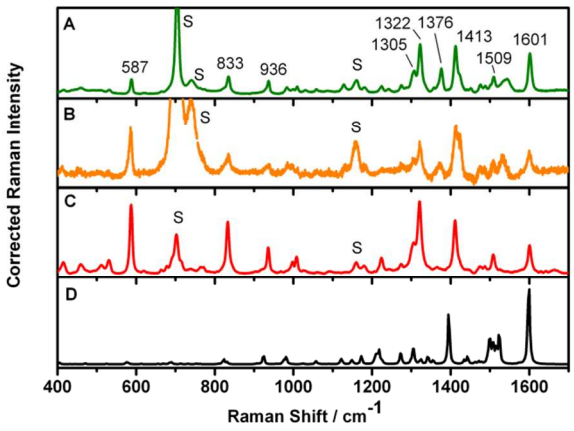

Figure 6. Resonance Raman spectra of **Cu(L-aza)$_2$** in CH_2Cl_2 solution. **A.** 514 nm excitation, **B.** 568 nm excitation **C.** 633 nm excitation **D.** Calculated Raman spectrum. Solvent bands are marked with 'S'.

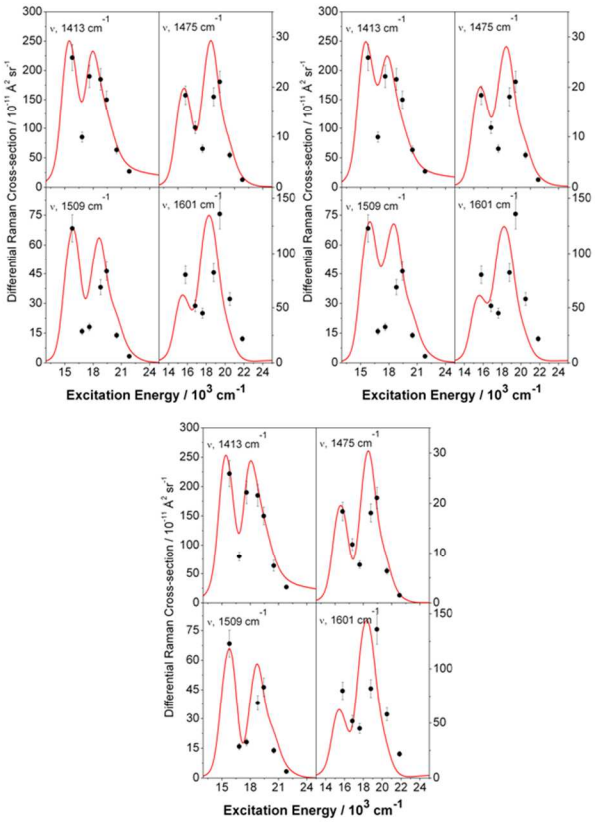

Figure 7. Simulated Raman Excitation Profiles and experimental Raman cross-section data for four selected vibrational modes. The Raman Excitation Profiles were simulated with values of $\alpha = 15^o$ (top, left), $\alpha = 45^o$ (top, right) and $\alpha = 85^o$(bottom).

quantum mechanical Raman scattering amplitudes from each state are summed and then squared to give the resonance Raman intensities (cross-sections), giving rise to interference effects that are sensitive to the angle between the transition dipole.[29] The 1413, 1475 and 1509 cm^{-1} profiles are particularly sensitive to the value of α, with the dip around 18 000 cm^{-1} increasing as the transition dipoles become orthogonal.

Table 2. Electronic parameters for **Cu(L-aza)$_2$**.obtained from simulation of absorption and Raman profiles. X_1 = low energy exciton state. X_2 = high energy exciton state. λ = outer-sphere (solvent) reorganization energy.

	X_1	X_2
E_{00} / cm^{-1}	14 425	16 725
μ / Å	0.918	1.03
λ / eV	0.086	0.117

For these modes the simulated profile for $\alpha = 85^o$ shows a much better fit to the experimental data than for $\alpha = 15^o$ or $\alpha = 45^o$. The resonance Raman data therefore supports two excited states with nearly orthogonal transition dipole moments, as suggested by the analysis of the TD-DFT output presented above. The same model for the electronic states is used to generate the absorption spectrum and resonance Raman profiles (the essential difference for the Raman profiles is the wavepacket motion is projected onto the individual vibrational wavefunctions). The absorption spectrum and the resonance Raman data then provide independent experimental verification of the exciton coupling model for **Cu(L-aza)$_2$**.

Our resonance Raman intensity analysis also provides dimensionless displacements along the resonant enhanced modes between the ground and excited-state geometries. The mode displacements provide a proxy for the electron displacement during the electronic transition. As discussed above the TD-DFT suggest that the orbitals involved in the electronic transitions have large amplitude on the pyrrole and phenyl ring atoms. This is entirely consistent with the mode displacements determined from the resonance Raman intensity analysis. The modes with the largest displacements are given in Table 3 along with qualitative mode descriptions. Table 3 shows that pyrrole and phenyl ring modes dominate the displacement caused by exciton creation in **Cu(L-aza)$_2$**. The mode displacements are also consistent with the orientation of the transition dipoles as suggested by the TD-DFT output and spectroscopic data. Phenyl ring modes also dominate the resonance Raman spectra of ruthenium dipyrrin complexes, and the excited-state dynamics of metallodipyrrins are controlled to a large extent by the transannular torsion of the phenyl rings.[26] The mode displacements map the dynamics of the excited-state wavepacket in the Franck-Condon region, *i.e.* within the first few fs following photoexcitation, and as such the resonance Raman spectra provide complementary information to ultrafast studies of photodynamics. Although ultrafast studies of azadipyrrins have been reported, these studies focus on donor-acceptor photoinduced electron transfer and utilize systems with single azadipyrrin chromophores.[45-47] We are not aware of any ultrafast studies of

Table 3. Vibrational mode parameters for **Cu(L-aza)$_2$** obtained from simulation of absorption and Raman profiles. X_1 = low energy exciton state. X_2 = high energy exciton state.

Mode[a]	ν / cm^{-1}	Δ_{X1}[b,d]	Δ_{X2}[b,d]	Mode Description[c]
91	587	1.0	0.30	phenyl ring distortion (CCC angle)
139,143	833	0.75	0.55	pyrrole-phenyl transannular torsion
158	936	0.5	0.5	phenyl ring torsion
251	1322	0.85	0.75	pyrrole ring antisymm stretch (C-N bond)
255	1376	0.25	0.35	pyrrole-phenyl CC bond stretch
257	1413	0.55	0.45	pyrrole ring breathing (symm stretch)
277	1509	0.40	0.40	pyrrole ring antisymm stretch (C-C bond)
293	1601	0.20	0.60	phenyl ring stretch

a. Mode number is taken from normal coordinates from UB3LYP/6-31G(d) frequency output
b. Δ is the dimensionless displacement
c. Plots of atomic displacement vectors for each mode can be found in the supporting information. The strongly enhanced modes listed here all have A symmetry.

Cu(L-aza)$_2$ or related excitonic azadipyrrin systems. Our resonance Raman intensity analysis suggests that the excited-state dynamics of azadipyrrin complexes should also be strongly influenced by the structure of the phenyl substituents, analogous to the excited-state dynamics of dipyrrin compounds.[48, 49]

Reorganization Energies

Azadipyrrin complexes have been identified as potential n-type charge-carrier materials due to their low reorganization energies. A recent theoretical study calculated internal (inner-sphere) reorganization energies for oxidation and reduction of Zn(L-aza)$_2$ and other complexes.[11] The inner-sphere reorganization energy (in cm^{-1} units) for exciton generation for **Cu(L-aza)$_2$** can also be calculated directly from the vibrational mode displacements (Table 3 and supporting information), determined by the resonance Raman intensity analysis, using

$$\lambda_{inner} = \sum_i \nu_i \Delta_i^2$$

where ν_i is the vibrational mode wavenumber (in cm^{-1}) and Δ_i is the dimensionless mode displacement. We obtain 0.294 eV and 0.249 eV for the low and high energy exciton states respectively. Our analysis also provides the outer-sphere reorganization energy for exciton generation (Table 2), with 0.086 eV and 0.117 eV for the low and high energy states respectively. For hole transfer, the theoretical method of Senevirathna *et al*[11] calculates the reorganisation energy using

$$^{+}\lambda = E_0(Q_+) - E_0(Q_0) + E_+(Q_0) - E_+(Q_+)$$

where E is energy, Q is geometry and the subscripts 0 and + indicate a neutral and cationic state respectively (an analogous expression was used for electron transfer). A value of 0.081 eV was obtained for the total internal reorganization energy for electron and hole transfer for Zn(L-aza)$_2$. Although our experimental values relate to the process of exciton formation whereas the computational results of Senevirathna *et al*[11] apply to charge-carrier formation, it is reassuring that our estimates are in good agreement. In any case, our experimental values provide a useful benchmark for theoretical calculations of reorganization energies for exciton generation in azadipyrrin systems.

Conclusion.

The absorption spectrum and resonance Raman excitation profiles strongly support two excited-states with equal oscillator strengths for **Cu(L-aza)$_2$**. Analysis of the absorption and resonance Raman spectra of **Cu(L-aza)$_2$** using TD-DFT and wavepacket dynamics has shown that the excited-states of **Cu(L-aza)$_2$** are exciton states, with approximately orthogonal and co-planar transition dipole moments. The phenyl substituents play a key role in determining the electronic structure in **Cu(L-aza)$_2$**. We are currently applying this model to other homoleptic L-aza and dipyrrin complexes to determine if our simple model holds generally for dipyrrins and their aza analogues.

Acknowledgements
TMM thanks the MacDiarmid Institute for Advanced Materials and Nanotechnology for partial support of a PhD stipend. MRW thanks Massey University and the MacDiarmid Institute for Advanced Materials and Nanotechnology for financial support.

Notes and references

[a] Institute of Fundamental Sciences, Massey University, Palmerston North, New Zealand.
[b] Department of Chemistry, University of Otago, Dunedin, New Zealand.
[c] School of Chemical and Physical Sciences, Victoria University of Wellington, Wellington, New Zealand.

† A comment on the definition of "line of ligand centres" is required. If θ, α or τ are determined using structural parameters then it is appropriate to define the line of ligand (or molecule or chromophore) centres using structural elements (*i.e.* the ligand centres). However our analysis suggests that the transition dipoles themselves should define the line of ligand centres, and in this case "line of transition centres' is perhaps a more appropriate description. In some cases e.g. J-aggregates, the transition dipole moment and line of molecule centre coincides and there is no need for the distinction.

Electronic Supplementary Information (ESI) available: TD-UB3LYP output including structural parameters and electronic transition data, plots of atomic displacements for selected vibrational modes, images of selected KS orbitals, table of mode displacements used for wavepacket analysis. See DOI: 10.1039/b000000x/

1. T. E. Wood and A. Thompson, *Chem. Rev.*, 2007, **107**, 1831-1861.
2. A. Bessette and G. S. Hanan, *Chem. Soc. Rev.*, 2014, **43**, 3342-3405.
3. A. Loudet and K. Burgess, *Chem. Rev.*, 2007, **107**, 4891-4932.
4. G. Ulrich, R. Ziessel and A. Harriman, *Angew. Chem. Int. Ed. Engl.*, 2008, **47**, 1184-1201.
5. T. M. McLean, D. Cleland, K. C. Gordon, S. G. Telfer and M. R. Waterland, *J. Raman Spec.*, 2011, **42**, 2154-2164.
6. X. Ma, X. X. Jiang, S. W. Zhang, X. B. Huang, Y. X. Cheng and C. J. Zhu, *Poly. Chem.*, 2013, **4**, 4396-4404.
7. W. Senevirathna and G. Sauve, *J. Mater. Chem. C*, 2013, **1**, 6684-6694.
8. M. E. El-Khouly, A. N. Amin, M. E. Zandler, S. Fukuzumi and F. D'Souza, *Chem.-Eur. J.*, 2012, **18**, 5239-5247.
9. X. D. Jiang, Y. T. Fu, T. Zhang and W. L. Zhao, *Tetrahedron Lett.*, 2012, **53**, 5703-5706.
10. P. Batat, M. Cantuel, G. Jonusauskas, L. Scarpantonio, A. Palma, D. F. O'Shea and N. D. McClenaghan, *J. Phys. Chem. A*, 2011, **115**, 14034-14039.
11. W. Senevirathna, C. M. Daddario and G. Sauve, *J. Phys. Chem. Lett.*, 2014, **5**, 935-941.
12. A. Bessette, J. G. Ferreira, M. Giguere, F. Belanger, D. Desilets and G. S. Hanan, *Inorg. Chem.*, 2012, **51**, 12132-12141.
13. N. Deligonul and T. G. Gray, *Inorg. Chem.*, 2013, **52**, 13048-13057.
14. N. Deligonul, A. R. Browne, J. A. Golen, A. L. Rheingold and T. G. Gray, *Organometallics*, 2014, **33**, 637-643.
15. L. Gao, N. Deligonul and T. G. Gray, *Inorg. Chem.*, 2012, **51**, 7682-7688.
16. R. Sakamoto, S. Kusaka, Y. Kitagawa, M. Kishida, M. Hayashi, Y. Takara, M. Tsuchiya, J. Kakinuma, T. Takeda, K. Hirata, T. Ogino, K. Kawahara, T. Yagi, S. Ikehira, T. Nakamura, M. Isomura, M. Toyama, S. Ichikawa, M. Okumura and H. Nishihara, *Dalton Trans.*, 2012, **41**, 14035-14037.
17. A. Palma, J. F. Gallagher, H. Muller-Bunz, J. Wolowska, E. J. L. McInnes and D. F. O'Shea, *Dalton Trans.*, 2009, **38**, 273-279.
18. T. S. Teets, J. B. Updegraff, A. J. Esswein and T. G. Gray, *Inorg. Chem.*, 2009, **48**, 8134-8144.
19. D. V. Partyka, N. Deligonul, M. P. Washington and T. G. Gray, *Organometallics*, 2009, **28**, 5837-5840.
20. V. S. Thoi, J. R. Stork, D. Magde and S. M. Cohen, *Inorg. Chem.*, 2006, **45**, 10688-10697.
21. S. M. Cohen and S. R. Halper, *Inorg. Chim. Acta*, 2002, **341**, 12-16.
22. S. G. Telfer, T. M. McLean and M. R. Waterland, *Dalton Trans.*, 2011, **40**, 3097-3108.
23. M. Kasha, H. R. Rawls and M. A. El-Bayoumi, *Pure Appl. Chem.*, 1965, **11**, 22.
24. K. Servaty, E. Cauet, F. Thomas, J. Lambermont, P. Gerbaux, J. De Winter, M. Ovaere, L. Volker, N. Vaeck, L. Van Meervelt, W. Dehaen, C. Moucheron and A. Kirsch-De Mesmaeker, *Dalton Trans.*, 2013, **42**, 14188-14199.
25. M. R. Waterland, S. L. Howell and K. C. Gordon, *J. Phys. Chem. A*, 2007, **111**, 4604-4611.
26. T. M. McLean, D. M. Cleland, S. J. Lind, K. C. Gordon, S. G. Telfer and M. R. Waterland, *Chem.-Asian J.*, 2010, **5**, 2036-2046.
27. M. J. Frisch, G. W. Trucks, H. B. Schlegel, G. E. Scuseria, M. A. Robb, J. R. Cheeseman, G. Scalmani, V. Barone, B. Mennucci, G. A. Petersson, H. Nakatsuji, M. Caricato, X. Li, H. P. Hratchian, A. F. Izmaylov, J. Bloino, G. Zheng, J. L. Sonnenberg, M. Hada, M. Ehara, K. Toyota, R. Fukuda, J. Hasegawa, M. Ishida, T. Nakajima, Y. Honda, O. Kitao, H. Nakai, T. Vreven, J. A. Montgomery, J. E. Peralta, F. Ogliaro, M. Bearpark, J. J. Heyd, E. Brothers, K. N. Kudin, V. N. Staroverov, R. Kobayashi, J. Normand, K. Raghavachari, A. Rendell, J. C. Burant, S. S. Iyengar, J. Tomasi, M. Cossi, N. Rega, J. M. Millam, M. Klene, J. E. Knox, J. B. Cross, V. Bakken, C. Adamo, J. Jaramillo, R. Gomperts, R. E. Stratmann, O. Yazyev, A. J. Austin, R. Cammi, C. Pomelli, J. W. Ochterski, R. L. Martin, K. Morokuma, V. G. Zakrzewski, G. A. Voth, P. Salvador, J. J. Dannenberg, S. Dapprich, A. D. Daniels, Farkas, J. B. Foresman, J. V. Ortiz, J. Cioslowski and D. J. Fox, Wallingford CT, 2009.
28. A. M. Moran, D. S. Egolf, M. Blanchard-Desce and A. M. Kelley, *J. Chem. Phys.*, 2002, **116**, 2542 - 2555.
29. D. S. Egolf, M. R. Waterland and A. M. Kelley, *J. Phys. Chem. B*, 2000, **104**, 10727-10737.
30. B. Li, A. E. Johnson, S. Mukamel and A. B. Myers, *J. Am. Chem. Soc.*, 1994, **116**, 11039-11047.
31. T. S. Teets, D. V. Partyka, J. B. Updegraff and T. G. Gray, *Inorg. Chem.*, 2008, **47**, 2338-2346.
32. M. Broring, R. Kruger, S. Link, C. Kleeberg, S. Kohler, X. Xie, B. Ventura and L. Flamigni, *Chem.-Eur. J.*, 2008, **14**, 2976-2983.
33. B. Ventura, G. Marconi, M. Broring, R. Krugerb and L. Flamigni, *New J. Chem.*, 2009, **33**, 428-438.
34. J. Ahrens, B. Boker, K. Brandhorst, M. Funk and M. Broring, *Chem.-Eur. J.*, 2013, **19**, 11382-11395.
35. R. Kobayashi and R. D. Amos, *Chem. Phys. Lett.*, 2006, **420**, 106-109.
36. D. Jacquemin, E. A. Perpete, G. Scalmani, M. J. Frisch, R. Kobayashi and C. Adamo, *J. Chem. Phys.*, 2007, **126**, 144105.
37. D. Jacquemin, E. A. Perpete, G. E. Scuseria, I. Ciofini and C. Adamo, *J. Chem. Theory Comput.*, 2008, **4**, 123-135.

38. R. F. Fink, J. Seibt, V. Engel, M. Renz, M. Kaupp, S. Lochbrunner, H. M. Zhao, J. Pfister, F. Wurthner and B. Engels, *J. Am. Chem. Soc.*, 2008, **130**, 12858-+.
39. Z. L. Cai, M. J. Crossley, J. R. Reimers, R. Kobayashi and R. D. Amos, *J. Phys. Chem. B*, 2006, **110**, 15624-15632.
40. P.-A. Plötz, T. Niehaus and O. Kühn, *J. Chem. Phys.*, 2014, **140**, -.
41. B. Kociper and T. A. Niehaus, *J. Phys. Chem. C*, 2013, **117**, 26213-26221.
42. S. Chibani, B. Le Guennic, A. Charaf-Eddin, O. Maury, C. Andraud and D. Jacquemin, *J. Chem. Theory Comput.*, 2012, **8**, 3303-3313.
43. M. Alonso, T. Woller, F. J. Martin-Martinez, J. Contreras-Garcia, P. Geerlings and F. De Proft, *Chem.-Eur. J.*, 2014, **20**, 4931-4941.
44. S. J. Lind, K. C. Gordon and M. R. Waterland, *J. Raman Spec.*, 2008, **39**, 1556-1567.
45. V. Bandi, M. E. El-Khouly, K. Ohkubo, V. N. Nesterov, M. E. Zandler, S. Fukuzumi and F. D'Souza, *Chem.-Eur. J.*, 2013, **19**, 7221-7230.
46. V. Bandi, M. E. El-Khouly, V. N. Nesterov, P. A. Karr, S. Fukuzumi and F. D'Souza, *J. Phys. Chem. C*, 2013, **117**, 5638-5649.
47. A. N. Amin, M. E. El-Khouly, N. K. Subbaiyan, M. E. Zandler, M. Supur, S. Fukuzumi and F. D'Souza, *J. Phys. Chem. A*, 2011, **115**, 9810-9819.
48. H. L. Kee, C. Kirmaier, L. H. Yu, P. Thamyongkit, W. J. Youngblood, M. E. Calder, L. Ramos, B. C. Noll, D. F. Bocian, W. R. Scheidt, R. R. Birge, J. S. Lindsey and D. Holten, *J. Phys. Chem. B*, 2005, **109**, 20433-20443.
49. I. V. Sazanovich, C. Kirmaier, E. Hindin, L. Yu, D. F. Bocian, J. S. Lindsey and D. Holten, *J. Am. Chem. Soc.*, 2004, **126**, 2664-2665.

Exciton coupling is applied for the first time to successfully explain the excited-state structure of metalloazadipyrrins.